Biophysical Chemistry 199 (2015) 39–45

Contents lists available at ScienceDirect

Biophysical Chemistry

journal homepage: http://www.elsevier.com/locate/biophyschem

A novel data-driven algorithm to reveal and track the ribosome heterogeneity in single molecule studies

Haopeng Yang, Ming Xiao [1], Yuhong Wang *

University of Houston, 4800 Calhoun Rd, Houston, TX 77214, USA

HIGHLIGHTS

- The FRET signals at the single ribosome's peptidyl transfer center are studied.
- Inhomogeneous subpopulations are identified with a novel data-driven algorithm.
- The subpopulation exchange among each other spontaneously in 2 min time intervals.
- The exchange patterns suggest that the ribosomal and tRNA dynamics are correlated.

GRAPHICAL ABSTRACT

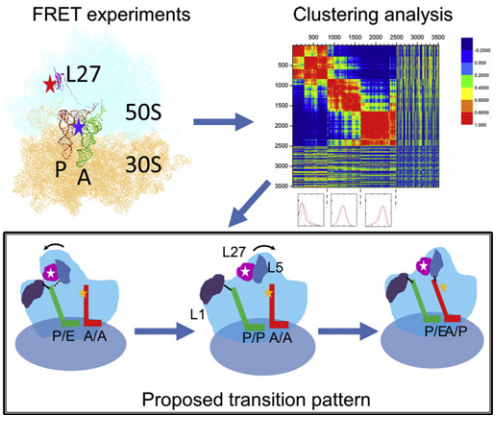

ARTICLE INFO

Article history:
Received 15 December 2014
Received in revised form 20 February 2015
Accepted 23 February 2015
Available online 3 March 2015

Keywords:
Ribosome conformational dynamics
Single molecule FRET
Data-driven algorithm
Dynamic heterogeneity

ABSTRACT

The unique advantage of the single molecule approach is to reveal the inhomogeneous subpopulations in an ensemble. For example, smFRET (single molecule fluorescence resonance energy transfer) can identify multiple subpopulations based on the FRET efficiency histograms. However, identifying multiple FRET states with overlapping average values remains challenging. Here, we report a new concept and method to analyze the single molecule FRET data of a ribosome system. The main results are as follows: 1. based on a hierarchic concept, multiple ribosome subpopulations are identified. 2. The subpopulations are self-identified via the cross-correlation analysis of the FRET histogram profiles. The dynamic heterogeneity is tracked after 2 min intervals on the same ribosomes individually. 3. The major ribosome subpopulations exchange with each other with a certain pattern, indicating some correlations among the motions of the tRNAs and the ribosomal components. Experiments under the conditions of 20% glycerol or 1 mM viomycin supported this conclusion.

1. Introduction

Single molecule methods track individual molecules in single reaction trajectories. Therefore, inhomogeneous subpopulations and rare reaction pathways can be observed in complex and out of phased biological systems, such as the ribosome system [1]. However, due to intrinsic fluctuations and instrumental noises, it is not always straightforward to

* Corresponding author. Tel.: +1 713 743 7941; fax: +1 713 743 8351.
E-mail address: ywang60@uh.edu (Y. Wang).
[1] Present addresses: Science China Press, Beijing 100717, China.

http://dx.doi.org/10.1016/j.bpc.2015.02.008
0301-4622/

extract kinetics and conformational information from a single molecule data. For example, in the single molecule fluorescence resonance energy transfer (smFRET), the subpopulations can be sorted by the FRET efficiency histograms or via the hidden Markov analysis for kinetic information [2]. Both methods are model-dependent and adding more states always helps them fit the data better. When the distributions of multiple FRET states are overlapped, the fitting becomes more biased by the initial parameters. Consequently, the kinetic information will not be reliable because it depends on the identification of FRET states. Here, we report a new model-free sorting method to identify the ribosome subpopulations.

The ribosome moves processively on the mRNA to assemble polypeptide. The aminoacyl tRNA pairs with the mRNA codon at the A-site and accommodates into the ribosome. Then, the elongating peptide chain on the P-site tRNA is transferred to the A-site tRNA via the new amide bond between the peptide chain and the aminoacyl tRNA. Afterward, the tRNAs move from the A- and P-sites to the P- and E-sites, respectively, which moves the next codon into the A-site for a new elongation cycle. The cycles continue until a stop codon moves into the A-site to finish the nascent peptide synthesis. Multiple ribosomal components and the tRNAs undergo large conformational changes during these processes [3,4]. The two subunits (30S and 50S) ratchet relative to each other; the 30S head swivels, and the tRNAs fluctuate between classical and hybrid binding positions in the 50S [5–9]. A cryo-EM study has identified more than 30 different subpopulations in the ribosome pre-translocation complex with different combinations of these movements, implying that the ribosome allosteric motions are not strongly correlated. On the other hand, it appears that more extensive inter-subunit ratcheting enables the tRNAs sample more conformations near their binding pockets, suggesting that the ribosome scaffolds dictate the tRNA dynamics [10]. In the meantime, we reported single molecule FRET studies on the ribosome that probed the distance between the A- or P-site tRNAs and the ribosomal protein L27. Three FRET states were observed at values of approximately 0.2, 0.47 and 0.68. However, the ribosomes cannot be simply assigned to only three states because individual ribosomes sample the three FRET states differently. Considering both values and dynamics of the FRET states, at least seven ribosome subpopulations can be identified: three subpopulations sample only one of the FRET states; three subpopulations sample only two of the three FRET states; and one subpopulation samples all three FRET states [11,12]. Therefore, more heterogeneity can be deduced, although not directly observable. This analysis method sorts the ribosome subpopulation based on a series of FRET data points instead of just one data point, therefore, the subpopulations identified are at a higher level of heterogeneity than the FRET values, which we have named the hierarchic model. The main difference between this hierarchic model and other methods is that both FRET values and dynamics are considered to define a subpopulation, whereas most other research reports define subpopulations only by the FRET values [13]. The hierarchic model agrees with the above-mentioned cryo-EM study that shows that the ribosome inter-subunit ratcheting conformations affect the tRNA dynamics. Similarly, the subpopulations identified by the hierarchic model are ribosomes with different conformations that allow different tRNA dynamics. However, our previous analysis still defines the FRET states via Gaussian fittings to the FRET efficiency histograms, which are biased by the initial guess values. In this report, the subpopulations are self-identified via cross-correlation analysis of the FRET efficiency histogram profiles. This analysis, therefore, eliminated the model-fitting of FRET states.

2. Results

2.1. Single molecule FRET experimental conditions

The FRET-paired dyes (Cy3–Cy5) are tethered on the C53 residue of the ribosomal protein L27 and the D-loop of the tRNA (D16/17), respectively, as described previously [11,14] (Fig. S1 and sample preparation description in the Supplemental material). In the pre-translocation complex, the dye-labeled $tRNA^{Phe}$ carrying the fMet–Phe dipeptidyl chain is at the A-site, while the vacant $tRNA^{fMet}$ is at the P-site (Fig. S1). The complex is tethered to the surface via the surface–streptavidin–biotin–mRNA interaction. A 532 nm laser is directed through a TIRF objective (Nikon Instruments) to illuminate the sample above the total internal reflection angle and generates an evanescent wave to excite the donor dye. The fluorescence emitted from the dyes are collected by the same objective and imaged on the CCD camera (Cascade II, Photometrics). The FRET efficiencies are calculated according to $E = I_{acceptor} / (I_{donor} + I_{acceptor})$. To remove signals with photophysical flickering, the fluctuation of the total fluorescent intensity ($I_{donor} + I_{acceptor}$) has to obey the Poisson distribution to warrant no donor photophysical flickering [15]. The acceptor physical flickering is tolerated because it occurs at a much lower frequency than the observed inhomogeneity [15]. Meanwhile, the signal noise level is set to less than 20%. For every ribosome, the fluorescence intensities are collected for 3 segments at 2 min intervals. Every segment contains 200 data points at 100 ms time resolution (Fig. 1, top panel). The FRET efficiencies are calculated (Fig. 1, second panel) and binned in 20 intervals between 0.02 and 1.02 to generate the histogram (Fig. 1, third panel). In the 2 min intervals, we have observed subpopulation transitions, which means that these conformational changes occur at the order of minutes. This time scale is slow compared with the 10–20 s^{-1} peptide elongation with elongation factors, but is fast compared with a factor-free spontaneous protein synthesis ($<0.03\ min^{-1}$) [16,17].

2.2. Identify the subpopulations

The FRET efficiency histograms obtained from individual ribosomes exhibit large heterogeneity. Fig. 2 displays 6 ribosome traces of the first time segment. The traces in the top panel prefer the low FRET state and sample the other FRET states much less frequently; the traces in the bottom panel sample the high FRET states most of the time. In a conventional analysis, these traces are pooled together, and an overall Gaussian-fitting of the total FRET efficiency histogram will generate several FRET states (Fig. S2). This analysis method is model-dependent and has ignored the heterogeneity of every trace. On the other hand, although no two traces are exactly the same, it is obvious that traces can be grouped based on the similarity of the FRET histogram profiles, such as the two panels in Fig. 2. This is reasonable because the FRET signal reflects the dynamics of the A-site tRNA that are dependent on the ribosome scaffolds. Therefore, similar FRET histogram profiles imply similar ribosome scaffolds. For example, in the ratcheted and non-ratcheted ribosome, the tRNA prefers the hybrid (high FRET state) and classical (low FRET state) binding sites respectively (Fig. S1 shows the expected FRET values and the tRNA configurations based on X-ray information [11]). Accordingly, ribosomes generating similar FRET histogram profiles are grouped as one subpopulation. Here, the definition of a subpopulation is not only the FRET values, but also the sampling frequencies among the states that indicate the relative energy gaps. The FRET dynamics are measured at 100 ms interval for 20 s (200 data points). Therefore, the subpopulations defined here are at a higher level than the FRET states only, and include the heterogeneity of single traces.

The FRET histogram profile similarity is quantified by the Pearson's cross-correlation coefficients among traces as shown in Fig. 2. Fig. 3 displays plots of the coefficient matrices of ribosomes under three experimental conditions: (a) in aqueous buffer solution (3519 traces); (b) in 20% glycerol buffer solution (1908 traces); (c) in the presence of viomycin in aqueous buffer (673 traces). For example, Fig. 3a is a matrix of 3519×3519 elements. For each element $M_{i,j}$, the value is the Pearson's correlation between the "ith" and "jth" traces. Therefore, the matrix is symmetric along the diagonal line because M_{ij} equals M_{ji}, and the values

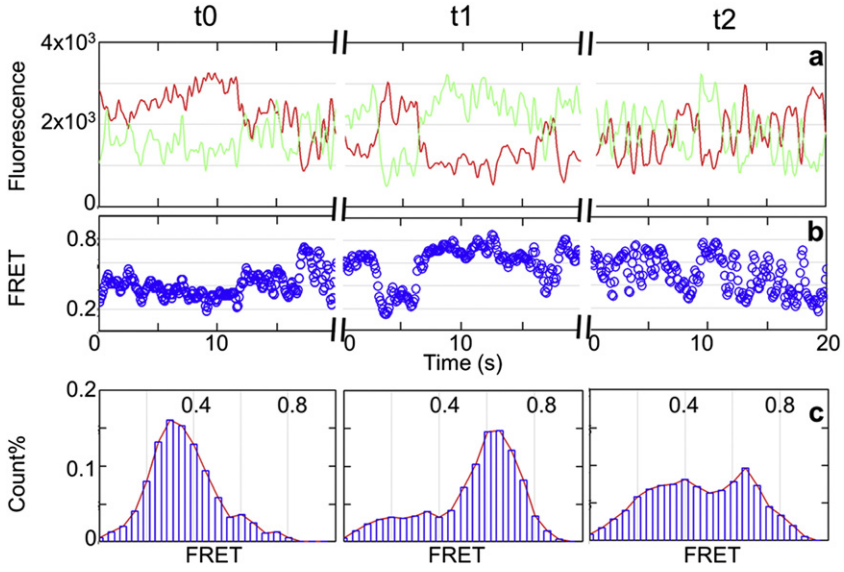

Fig. 1. Single molecule FRET data and generation of the FRET efficiency histogram. (a) The fluorescence intensities of the donor and the acceptor in three segments of 20s acquisition windows. The time interval between consecutive segments is 2 min. In each segment, the data is collected at 100 ms/frame. (b) The calculated FRET efficiency from the fluorescence intensities by $E = I_{acceptor} / (I_{donor} + I_{acceptor})$. (c) The FRET efficiency histograms of the FRET efficiency traces in (b). The range of the histogram is 0.02–1.02. The total counts are normalized to 1.

on the diagonal line are "1" because the correlations between the same traces are 100%. The coefficient matrices are then color-coded. The subpopulations are identified by the self-separated blocks on the plots. The red-colored blocks off the diagonal show high correlation coefficients among subpopulations. This means that there are traces correlated with both groups above the threshold that can be clustered in either one. As the kinetic simulations show in the Supplementary material, the lifetimes of the subpopulations are on the order of the acquisition window. Therefore, some ribosomes may transit from one subpopulation to another during the acquisition, which makes their traces correlate with both groups.

The data analysis to arrange the traces into clusters is as follows. First, traces are grouped in small clusters such that any two traces in the same cluster correlate with a coefficient larger than 0.9. Then, the average FRET histogram profiles from each cluster are used to generate a coefficient matrix. The matrix is re-organized similar to the dendrogram [18]. Afterward, the average traces are replaced by the original traces at the re-organized positions. Finally, the subpopulation groups are re-ordered by their average FRET histogram profiles' peak positions from low to high. The subpopulations are identified by the naturally formed interfaces between different blocks in Fig. 3. The threshold to be in the same subpopulation is set to be >0.85. Higher or lower thresholds will identify more or fewer subpopulations. The averaged FRET histograms of the major subpopulations are displayed at the bottom of each correlation matrix in Fig. 3 and overlaid together in Fig. 4. There are in total 6 significant subpopulations (marked G1–G6). Compared with the overall-fitting method (fitting results shown in Fig. S2), more FRET states can be identified without prior-set models.

2.3. Track exchanges among subpopulations

The subpopulations at the first 20 s (t_0) observation window are tracked after 2 min for another 20 s observation (t_1). For example, the correlation matrix of the 556 ribosomes of G2 group at t_0 (Fig. 5a) changes into multiple subpopulations as shown in Fig. 5b. The major subpopulations that count for 66% of the original G2 group are shown in Fig. 5c (11% of G1, 35% of G2, 17% of G3, and 3% of G4). Approximately 12% of the ribosomes form small-numbered groups as shown in Fig. 5d (2.2% of Gx1, 3.2% of Gx2, 3.2% of Gx3, and 3.4% of Gx4). These groups may be the short-lived intermediate states between the major subpopulations because the FRET histograms exhibit more than one well-separated peak, while the major groups in Fig. 4 exhibit mostly one major peak. Approximately 10% of the ribosomes cannot cluster with any group, Fig. 5d shows some examples. In addition, the rest of the

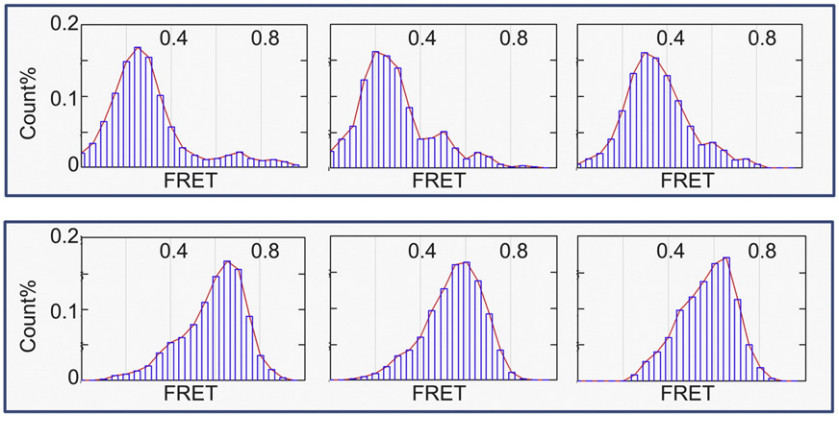

Fig. 2. Examples of diverse ribosome FRET efficiency histograms. Each plot represents one ribosome FRET histogram in 20 s acquisition window. The examples in the top and the bottom panels are different to each other. But within each panel, the histograms are similar.

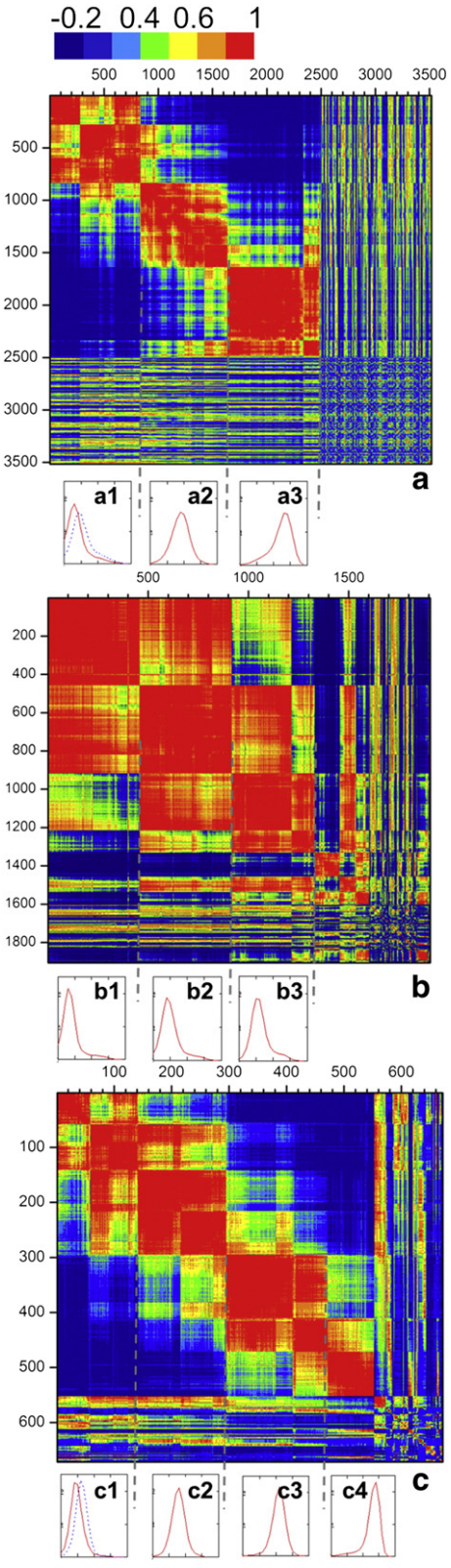

Fig. 3. The correlation matrices of the FRET histograms in three conditions: (a) plain buffer; (b) 20% glycerol; and (c) plain buffer + 1 mM viomycin. The subpopulations are identified by the self-assembled blocks. The dashed lines indicate the borders of subpopulations. The average FRET histogram profiles of each subpopulation are displayed at the bottom of each subpopulation block (labeled as a1–3, b1–3 and c1–4, respectively). In plots a1 and c1, two FRET histogram curves (G1 and G2) are displayed together to distinguish them more obviously. The subpopulations are re-plotted in Fig. 4.

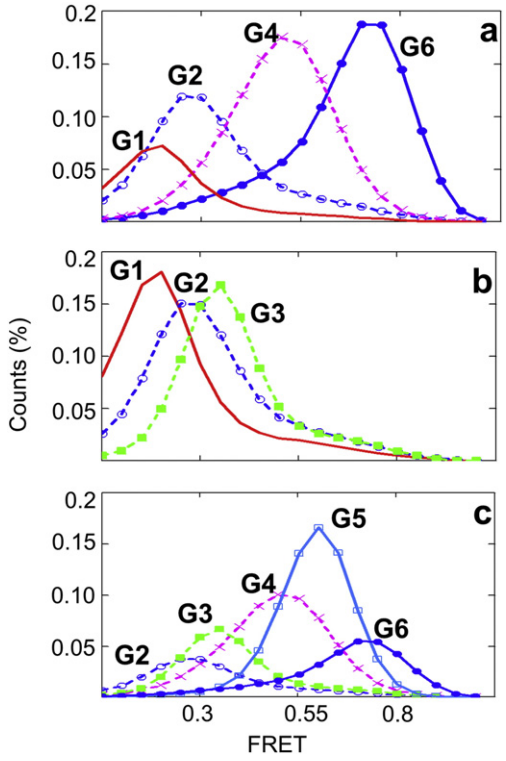

Fig. 4. Subpopulations that are identified from the cluster analysis in Fig. 3: (a) plain buffer; (b) 20% glycerol; and (c) plain buffer + 1 mM viomycin. The curves are normalized to their relative abundance. Figure legends: (—) G1, (o) G2, (■) G3, (x) G4, (□) G5, and (●) G6.

ribosomes have bleached at t_1. The transition matrices for all of the major subpopulations are summarized in Table S1–3. In these tables, the first column displays the subpopulations at t_0 and the same row of the specific subpopulation displays the percentages of each subpopulation formed at t_1. Approximately 60–85% of the t_0 subpopulations is accounted for at t_1, the rest transit to subpopulations that are not statistically significant but may be short-lived intermediates, such as those in Fig. 5d.

3. Discussion

3.1. A model of ribosome spontaneous exchange

The transition matrix of Table S1 suggests a sequential transition from the low FRET (0.2–0.3) to the high FRET peaks (0.7) via the medium (0.35–0.6) peaks. In the presence of glycerol or viomycin, the transitions are biased toward the subpopulations favoring the low or medium FRET states, respectively (Tables S2 and S3, Fig. S2). Fig. 6 summarizes the transition. The subpopulations can be correlated to the ribosome structures because the FRET values reveal the tRNA configurations. Fig. S1 shows that the FRET-paired dyes are tethered on the L27 and the A-site tRNA, respectively. In the classical state, the tRNAs are in the A/A and the P/P configurations, in which the letters before and after the slash stand for the tRNA binding sites in the small and large subunits, respectively. In the putative hybrid state [19], the tRNAs move in the large subunit but remain stable in the small subunit to form the A/P and P/E configurations. Because the distance between the P-site bound tRNA and the L27 is shorter than the distance between the A-site bound tRNA and the L27, the A/P configuration generates a higher FRET value. On the other hand, a second hybrid state can be formed in which the tRNAs are in the A/A and P/E configurations. To assist the formation of this state, the ribosome central protuberance swings toward the E-site [10,20]. Because the L27 is in the central protuberance, this

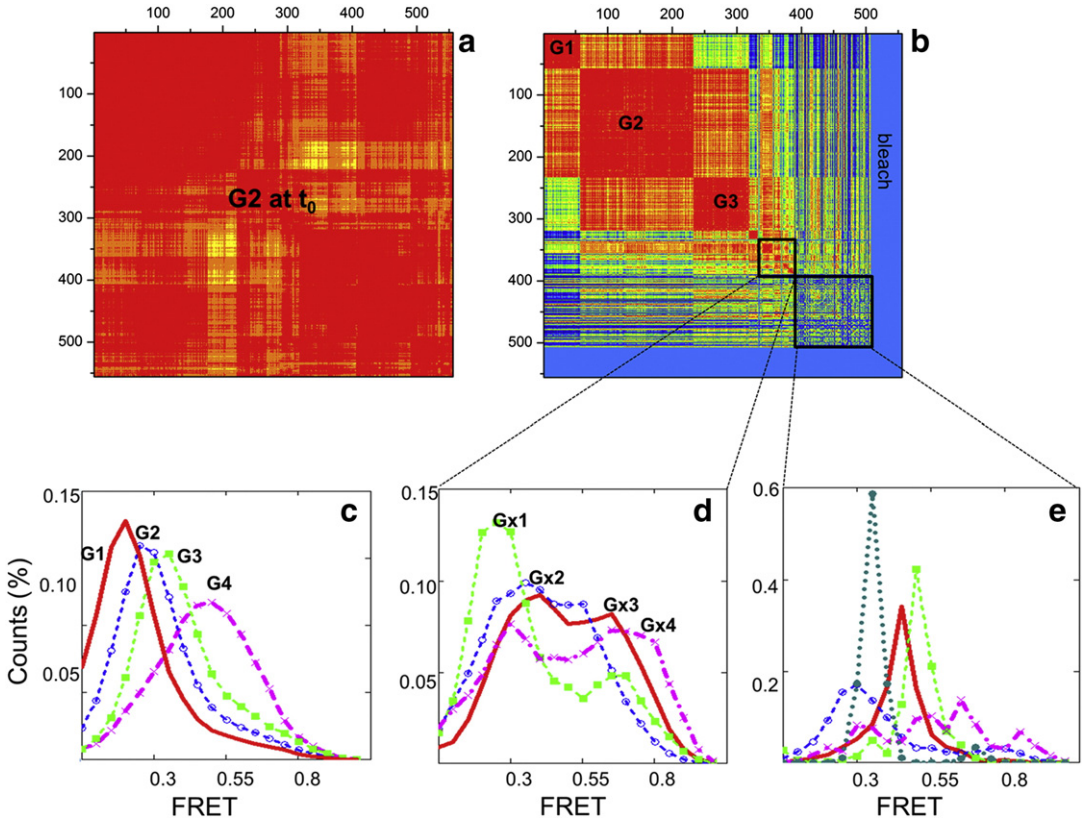

Fig. 5. An example of subpopulation transition. (a) The correlation matrix of G2 group at t_0. (b) The correlation matrix of G2 at t_1 after clustering analysis. The sum of G1–G4 accounts 66% of the total ribosomes. (c) The profiles of the major subpopulations are shown: the legends are the same as in Fig. 4. (d) The profiles of the low-percentage subpopulations. (e) Examples of traces that do not cluster with any groups.

hybrid state exhibits a lower FRET value than the classical state. The schematic illustration of all three tRNA conformations is shown in Fig. S1. Accordingly, we propose the assignment of the subpopulations (G1–G2) that prefer the low FRET states to the ribosomes with the central protuberance swinging toward the E-site. The subpopulations (G3–G5) that refer the medium FRET states are assigned to the ribosome with normal central protuberance position and non-ratcheted inter-subunit orientation. The subpopulation (G6) that prefers the high FRET states is assigned to the ribosome with normal central protuberance position and ratcheted inter-subunit orientation because ratcheted ribosome conformation is essential to form the tRNA hybrid states [5–7,21]. These assignments are consistent with the viomycin and glycerol experiments. As shown in Fig. 4, the G6 subpopulation that prefers the high FRET state is suppressed by viomycin, because in the presence of viomycin, the ribosome is in the non-ratcheted conformation [22]. On the other hand, 20% glycerol increases the buffer solution viscosity approximately 2-fold, which is similar to the cytoplasm's viscosity [23]. The high viscosity has been shown to slow down the protein conformational change significantly [24]. The viscosity may have a larger effect on ribosome inter-subunit ratcheting than internal motions within a subunit because the larger scale movements are during the inter-subunit ratcheting. Therefore, G1–3 subpopulations are favored but G6 is disfavored in 20% glycerol buffer solution. These structural analyses suggest that the ribosome subpopulations determine the tRNA dynamics. On the other hand, the transitions of the subpopulations are correlated with the tRNA configurations from low to high FRET values, which means that the tRNA motions also guide the ribosome conformational change in a biased direction in contrast to an entirely random walk.

3.2. The effect of time window of acquisition

To analyze whether the subpopulations and their exchange patterns depend on the specific time window (20 s), we have analyzed the data of plain buffer experiments with 5 and 10 s (Fig. S3). In this analysis, the FRET histograms are generated as in Fig. 1, except only the first 50 or 100 points are used. Figs. S3b and S3c show the cross-correlation matrices of the FRET histograms of 10 s or 5 s to that generated with 20 s. Fig. S3a is the auto-correlation matrix of the 20 s data. In addition, Figs. S3d and S3e are the autocorrelation matrices of the 10 s and 5 s data, respectively. In all of Fig. S3b–e, the traces remain in the same order as those in Fig. S3a without re-grouping and the color codes are the same as in Fig. 3. The clusters are still obvious in all these plots, although the correlation efficiencies are lower for 5 s and 10 s data. This is because the shorter acquisition window decreases the probability of subpopulation transitions during the data collection time. Meanwhile, fewer data points cause higher shot-noises that decrease the correlation coefficients. Figs. S3f and S3g are the correlation matrices of the 10 s and 5 s data after allowing the traces to re-group, using the same clustering analysis algorithm. The overall groups are consistent with those in Figs. 3a and S3a. The average FRET histogram profiles are exactly the same as those shown in Fig. 4a. Not surprisingly, fewer traces are grouped in each cluster because of the shorter acquisition time, which are shown in Tables S4 and S5. These tables also show the subpopulation transition matrices using the 10 s and 5 s data, which agree with the pattern shown in Table S1. These analyses indicate that the length of the data window does not interfere with the main conclusions here.

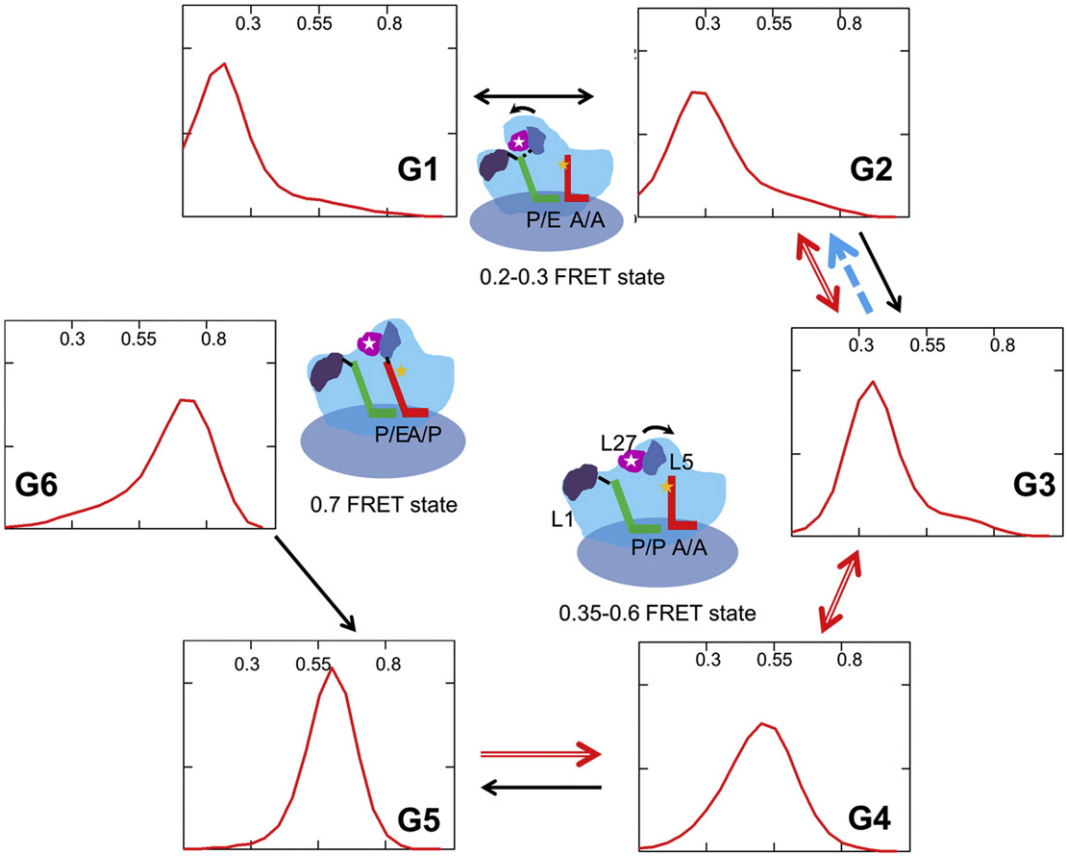

Fig. 6. The transition pattern of the major subpopulations under the three experimental conditions. The solid arrows are transitions in aqueous buffer; the dashed arrow is the transition in 20% glycerol solutions; and the double-lined arrows are transitions in the presence of viomycin.

3.3. The effect of waiting time between acquisitions

The same ribosomes are tracked at 2 min and 4 min intervals (Fig. 1). The subpopulation transition matrices are tabulated in Tables S1 and S6, respectively. There is no dramatic difference in these two tables, which suggests that the 2 min interval is sufficient to reach the exchange equilibrium. Using the kinetic scheme in Fig. 6 and the transition matrix in Tables S1 and 3, the kinetics of the subpopulation exchanges are simulated (Supporting information and Fig. S4). The simulation step (time unit dt) is set to be the interval of 1% decay of G1. Fig. S4 shows that after approximately 1000 steps the subpopulations reach an equilibrium. Assuming 2 min is the time of 1000 steps (1000 dt), the lifetime of the subpopulations is calculated to be 12.5 s ($k = 0.08\ s^{-1}$). This lifetime is comparable to the 20 s acquisition window, which may be a reason for the high correlations between the neighboring subpopulations. On the other hand, the transition rate cannot be too fast during the 20's acquisition window. If the transitions are very fast, all of the ribosomes will sample all of the subpopulations within 20 s. The correlations of different ribosomes should be high to cluster to only one population. Conversely, no static heterogeneity should be detected. This is the opposite of what we have observed. Considering this observation and the reasonable consistency between the simulation and experiments, the estimation of the subpopulation lifetimes are most likely close to the true values.

4. Conclusion

We have analyzed the single molecule FRET data with a hierarchic subpopulation concept and the clustering analysis tool. Using this method, we have identified more ribosome subpopulations without pre-set models. The exchanges among these subpopulations after 2 min and 4 min are tracked and shown to follow a certain pattern. On the other hand, the experiments with glycerol, which mimics the cell viscosity, indicate that fewer ribosome subpopulations are sampled. This observation implies that solution viscosity has an impact on the ribosome conformational flexibility compared with the aqueous buffers in which most in vitro experiments are conducted in the literature.

Acknowledgment

This work is supported by the Welch Foundation (E-1721) and NHARP of Texas (003652-0010-2011) to Y.W.

Appendix A. Supplementary data

Supporting information including 4 figures, 6 tables, description of sample preparation and kinetic simulations. Supplementary data associated with this article can be found, in the online version, at http://dx.doi.org/10.1016/j.bpc.2015.02.008.

References

[1] S. Chu, Biology and polymer physics at the single-molecule level, Philos. Transact. A Math. Phys. Eng. Sci. 361 (2003) 689–698.
[2] M. Blanco, N.G. Walter, Analysis of complex single-molecule FRET time trajectories, Methods Enzymol. 472 (2010) 153–178.
[3] R.K. Agrawal, A.B. Heagle, P. Penczek, R.A. Grassucci, J. Frank, EF-G-dependent GTP hydrolysis induces translocation accompanied by large conformational changes in the 70S ribosome, Nat. Struct. Biol. 6 (1999) 643–647.
[4] H. Stark, M.V. Rodnina, H.J. Wieden, M. van Heel, W. Wintermeyer, Large-scale movement of elongation factor G and extensive conformational change of the ribosome during translocation, Cell 100 (2000) 301–309.

[5] J. Zhou, L. Lancaster, J.P. Donohue, H.F. Noller, Crystal structures of EF-G-ribosome complexes trapped in intermediate states of translocation, Science 340 (2013) 1236086.
[6] D.S. Tourigny, I.S. Fernandez, A.C. Kelley, V. Ramakrishnan, Elongation factor G bound to the ribosome in an intermediate state of translocation, Science 340 (2013) 1235490.
[7] A. Pulk, J.H. Cate, Control of ribosomal subunit rotation by elongation factor G, Science 340 (2013) 1235970.
[8] A.H. Ratje, J. Loerke, A. Mikolajka, M. Brunner, P.W. Hildebrand, A.L. Starosta, A. Donhofer, S.R. Connell, P. Fucini, T. Mielke, P.C. Whitford, J.N. Onuchic, Y. Yu, K.Y. Sanbonmatsu, R.K. Hartmann, P.A. Penczek, D.N. Wilson, C.M. Spahn, Head swivel on the ribosome facilitates translocation by means of intra-subunit tRNA hybrid sites, Nature 468 (2010) 713–716.
[9] J. Frank, R.K. Agrawal, A ratchet-like inter-subunit reorganization of the ribosome during translocation, Nature 406 (2000) 318–322.
[10] N. Fischer, A.L. Konevega, W. Wintermeyer, M.V. Rodnina, H. Stark, Ribosome dynamics and tRNA movement by time-resolved electron cryomicroscopy, Nature 466 (2010) 329–333.
[11] M.E. Altuntop, C.T. Ly, Y. Wang, Single-molecule study of ribosome hierarchic dynamics at the peptidyl transferase center, Biophys. J. 99 (2010) 3002–3009.
[12] Y. Wang, M. Xiao, Role of the ribosomal protein L27 revealed by single-molecule FRET study, Protein Sci. 21 (2012) 1696–1704.
[13] P.V. Cornish, D.N. Ermolenko, H.F. Noller, T. Ha, Spontaneous intersubunit rotation in single ribosomes, Mol. Cell 30 (2008) 578–588.
[14] C.T. Ly, M.E. Altuntop, Y. Wang, Single-molecule study of viomycin's inhibition mechanism on ribosome translocation, Biochemistry 49 (2010) 9732–9738.
[15] Y. Wang, M. Xiao, Y. Li, Heterogeneity of single molecule FRET signals reveals multiple active ribosome subpopulations, Proteins 82 (2014) 1–9.
[16] Y.P. Semenkov, T.G. Shapkina, S.V. Kirillov, Puromycin reaction of the A-site bound peptidyl-tRNA, Biochimie 74 (1992) 411–417.
[17] V.I. Katunin, A. Savelsbergh, M.V. Rodnina, W. Wintermeyer, Coupling of GTP hydrolysis by elongation factor G to translocation and factor recycling on the ribosome, Biochemistry 41 (2002) 12806–12812.
[18] S. Zadran, F. Remacle, R.D. Levine, miRNA and mRNA cancer signatures determined by analysis of expression levels in large cohorts of patients, Proc. Natl. Acad. Sci. U. S. A. 110 (2013) 19160–19165.
[19] D. Moazed, H.F. Noller, Intermediate states in the movement of transfer RNA in the ribosome, Nature 342 (1989) 142–148.
[20] L.V. Bock, C. Blau, G.F. Schroder, I.I. Davydov, N. Fischer, H. Stark, M.V. Rodnina, A.C. Vaiana, H. Grubmuller, Energy barriers and driving forces in tRNA translocation through the ribosome, Nat. Struct. Mol. Biol. 20 (2013) 1390–1396.
[21] J. Zhou, L. Lancaster, J.P. Donohue, H.F. Noller, How the ribosome hands the A-site tRNA to the P site during EF-G-catalyzed translocation, Science 345 (2014) 1188–1191.
[22] R.E. Stanley, G. Blaha, R.L. Grodzicki, M.D. Strickler, T.A. Steitz, The structures of the anti-tuberculosis antibiotics viomycin and capreomycin bound to the 70S ribosome, Nat. Struct. Mol. Biol. 17 (2010) 289–293.
[23] P.A. Valberg, H.A. Feldman, Magnetic particle motions within living cells. Measurement of cytoplasmic viscosity and motile activity, Biophys. J. 52 (1987) 551–561.
[24] A. Ansari, C.M. Jones, E.R. Henry, J. Hofrichter, W.A. Eaton, The role of solvent viscosity in the dynamics of protein conformational changes, Science 256 (1992) 1796–1798.